Dynare Working Papers Series

Stochastic Extended Path

Stéphane Adjemian
Michel Juillard

CEPREMAP
CENTRE POUR LA RECHERCHE ECONOMIQUE ET SES APPLICATIONS

STOCHASTIC EXTENDED PATH

STÉPHANE ADJEMIAN AND MICHEL JUILLARD

ABSTRACT. The Stochastic Extended Path (SEP) method enhances the traditional Extended Path technique by integrating numerical methods to estimate conditional expectations. In contrast to the deterministic Extended Path, which presumes that future shocks will align with their expected values, SEP accommodates stochastic nonlinearity by performing integration over future shocks. We employ numerical techniques, including Gaussian quadrature and unscented transforms, to efficiently approximate integrals while alleviating the challenges posed by the curse of dimensionality. To further enhance accuracy, we propose a hybrid strategy that merges SEP with perturbation methods to effectively address long-run uncertainty effects. We evaluate the performance of SEP in an asset pricing model with a closed-form solution and demonstrate the methodology using a Real Business Cycle (RBC) model featuring irreversible investment.

INTRODUCTION

The extended path approach, initially introduced by Fair and Taylor (1983) and implemented in Dynare, utilizes perfect foresight model solvers to effectively address deterministic nonlinearities related to preferences, technology functional forms, or occasionally binding constraints. In each period of the simulation, exogenous innovations are treated as surprise shocks occurring in the first period of a deterministic simulation, with shocks thereafter set to their expected values. This approach offers significant advantages over other global approximation methods, including the ability to simulate very large models and its simplicity, as it is not model-dependent and requires no more effort than composing a Dynare *.mod file.

This approach, which relies on perfect foresight model solvers, inherently overlooks Jensen's inequality. While the extended path method can handle deterministic nonlinearity with arbitrary precision, it remains unaddressed regarding stochastic nonlinearity. Since future shocks are anticipated to equal their expectations, current agent behavior is unaffected by future uncertainty. According to Gagnon (1990) and Love (2009), who analyze an RBC model, this approximation has minimal effects. However, Adjemian and Juillard (2011) demonstrated, in the context of an NK model with a zero lower bound on nominal interest rates, that neglecting future uncertainty is inconsequential only when the interest rate constraint is non-binding. In this paper, we

propose relaxing the assumption about future shocks by employing numerical integration to approximate conditional expectations.

The Stochastic Extended Path approach (SEP), similar to the deterministic Extended Path approach, generates time series for the model's endogenous variables without explicitly calculating a reduced form that links choice variables to state variables[1]. This method is advantageous in cases where the model's reduced form is poorly behaved due to high non-linearity or kinks, which makes it challenging to approximate. However, a drawback is that it does not leverage the problem's recursive structure, limiting its ability to fully account for future uncertainty. Specifically, it requires integration over shocks in all future periods, which may not be feasible[2]. The Stochastic Extended Path of order p simplifies future uncertainty by positing that shocks will occur in the next p periods, with subsequent shocks set to their expected values. Agents then expect that the economy goes back to the deterministic steady state.

Section 1 introduces the class of models being examined and the Extended Path approach. Section 2 addresses modifications to the Extended Path approach to incorporate the impact of future uncertainty. Additionally, we conduct accuracy checks using a model where future uncertainty is significant and for which a closed-form solution is available. Section 3 presents a numerical illustration considering a Real Business Cycle (RBC) model with irreversible investment.

1. EXTENDED PATH

We assume that the model can be expressed in the following manner:

$$(1) \qquad \mathbb{E}_t \left[f \left(y_{t-1}, y_t, y_{t+1}, \varepsilon_t \right) \right] = 0$$

where y_t is an $n \times 1$ vector of endogenous variables, ε_t is a $n_s \times 1$ random vector of innovations, and $f : \mathbb{R}^{3n+n_s} \to \mathbb{R}^n$ is a continuous function. The innovations are assumed to be independent and identically distributed and follow a Gaussian distribution: $\mathcal{N}(0, \Sigma)$. The assumption regarding the distribution of innovations can be relaxed; however, this would necessitate the use of different numerical integration rules in section 2. The conditional expectation is presented above the function f, but we could readily extend this to consider conditional expectations under a nonlinear function by incorporating additional auxiliary variables. Similarly, we could address an arbitrary number of lags or leads by utilizing auxiliary variables. We do not assume that the function f is differentiable everywhere, which is why the extended path approach can accommodate scenarios where the left and right derivatives differ due to occasionally binding constraints. Nevertheless, it is evident that solving a model is

---

[1]Note however that, in a subsequent stage, one can estimate this relationship using the time series generated by the SEP approach. The fitted polynomial can serve as an initial guess for the Parameterized Expectations Algorithm or be used to extend the simulation with significantly reduced computational costs.

[2]Note that the pertubation approach fully account for future uncertainty conditionally on a given approximation order, in this sense it does not account for all the future uncertainty.

always easier when f is differentiable at all points[3]. We also assume that the model has a deterministic steady state and that the economy converges to this steady state in the long run. There exists a vector of endogenous variables $y^\star$ such that:

$$f(y^\star, y^\star, y^\star, 0) = 0$$

and $\lim_{h \to \infty} y_{t+h} = y^\star$ for all y_{t-1}. This assumption could be relaxed; what is essential is a terminal condition for the endogenous variables. As long as we know where the economy goes in the long run (for instance, along a balanced growth path), the method described below can be accommodated.

1.1. **Perfect foresight model.** Perfect foresight models are commonly employed to generate impulse response functions. Starting with an initial condition y_{t-1} and an unexpected shock occurring in period t, ε_t, we aim to find the trajectory of the endogenous variables under the assumptions that *(i)* subsequent shocks are set to their expected values, *(ii)* the model reaches the steady state y^* in period $t + H$.

(2)
$$\begin{cases} f(y_{t-1}, y_t, y_{t+1}, \varepsilon_t) = 0 \\ f(y_{t-1+h}, y_{t+h}, y_{t+h+1}, 0) = 0 & \forall h = 0, \ldots, H-2 \\ f(y_{t+H-2}, y_{t+H-1}, y^\star, 0) = 0 \end{cases}$$

Comparing this system of equations to equation (1), assumption *(i)* suggests that it is legitimate to pass the expectation operator inside the function f. This is obviously a crude approximation, since f is a priori a non-linear funtion. Assumption *(ii)* is less concerning, as the distance to the steady state can be made arbitrarily small with a sufficiently large simulation horizon, H.

Concatenating all the vectors of endogenous variables in the $nH \times 1$ vector $Y_t = (y_t', y_{t+1}', \ldots, y_{t+H-1}')'$ the system of equations to be solved can be written as:

$$F(Y_t) = 0$$

where $F : \mathbb{R}^{nH} \to \mathbb{R}^{nH}$ is a function that aggregates the functions f across all periods. Laffargue (1990) demonstrates that perfect foresight models can be solved using Newton-type methods, taking advantage of the sparse structure of the Jacobian of F, which is block tridiagonal. In the Newton approach, the solution for vector Y is found iteratively. For an initial guess $Y_t^{(0)}$, usually the steady state or a path generated by a first order apporoximation of the model, successive approximated solutions $Y_t^{(k)}$ are obtained by solving the following linear problem:

$$F\left(Y_t^{(k)}\right) + J_F\left(Y_t^{(k)}\right)\left(Y_t^{(k+1)} - Y_t^{(k)}\right) = 0$$

---

[3]When calculating the derivatives of an equation that includes the binary operators max or min, Dynare returns the derivative of the first argument in the event of a tie between the two arguments. This behavior can lead to a deterministic simulation failing with $\max(\varphi(y), \psi(y))$ while succeeding with $\max(\psi(y), \varphi(y))$ in an equation.

where $J_F\left(Y_t^{(k)}\right)$ is the Jacobian matrix of F evaluated at the current trajectory for the endogenous variables $Y_t^{(k)}$. With current computers, standard algorithms for solving sparse linear problems, such as those developed by Davis (2006), and available in Matlab or Octave, for example, can be used very efficiently in this framework.

1.2. **Extended path algorithm.** To simulate stochastic models, Fair and Taylor (1983) propose the following approach: for each period in the stochastic simulation, draw a random vector of stochastic shocks ε_t; run an auxiliary deterministic version of the model[4], assigning the shocks in the first period to ε_t while setting all future shocks to zero; then, use the values of the endogenous variables from the first period of this auxiliary model as the values of the endogenous variables in period t of the stochastic simulation. Below is a sketch of the algorithm:

Algorithm 1 Extended path algorithm

---
1. $H \leftarrow$ Set the horizon of the perfect foresight models
2. $y_0 \leftarrow$ Choose an initial condition
3. **for** $t = 1$ to T **do**
4. $\varepsilon_t \leftarrow$ Draw a random vector from a gaussian distribution $\mathcal{N}(0, \Sigma)$
5. $y_t \leftarrow$ Solve the auxiliary perfect foresight model using y_{t-1} as the initial condition, with the terminal condition $y_{t+H} = y^\star$
6. **end for**

In iteration t of the main loop, the initial guess for the auxiliary perfect foresight model solver is constructed from the solution of the same model in step $t-1$. In this approach, conditional expectations are approximated by setting the shocks to zero, their expected value. This method overlooks Jensen's inequality and simulates a stochastic scenario based on a form of certainty equivalence. Whether this poses a problem depends on the specific model being used. In this model, agents operate under the premise that future shocks will not occur. However, in each subsequent period, they encounter new non-zero realizations of these shocks. Despite facing these fluctuations, they gain no insights about the future uncertainty from their experiences in each period. It is important to note that a perturbation approach based on a first-order approximation of the model would encounter similar limitations, failing to address the deterministic nonlinearity inherent in the model. In contrast, the Extended Path approach accepts certainty equivalence as a trade-off for comprehensively accounting for the deterministic nonlinearity. Another advantage of this approach is its ability to accurately simulate models with variables that significantly deviate from the deterministic steady state, where perturbation methods would yield inaccurate solutions. Finally, in contrast to perturbation-based solutions, this approach enables the incorporation of an arbitrary number of occasionally binding constraints, as we do not require

---
[4]It is important to note that we employ a relaxation method to solve the perfect foresight auxiliary model in Dynare, while Fair and Taylor (1983) utilized a shooting method, which is known to be less efficient.

the differentiability of f.

The Extended Path approach allows for the simulation of large models with arbitrary precision, as the number of required operations increases only polynomially with the number of endogenous variables (the primary task when solving the auxiliary perfect foresight model consists in solving a sparse system of linear equations). This contrasts with a global approximation of the policy rules or expectations, where the complexity grows exponentially. The Extended Path approach is not affected by the so-called curse of dimensionality concerning the number of state variables.

2. Stochastic Extended Path

To accommodate non-zero shocks in periods $t + 1$, $t + 2$, $\ldots$, $t + p$ ($p \geq 1$), it is necessary to explicitly compute the (conditional) expectations for the periods t, $t + 1$, $\ldots$, $t + p - 1$. We begin by outlining various approaches employed in Dynare for approximating integrals. Next, we detail the computation of conditional expectations. Following that, we assess the stochastic extended path approach by comparing its results with those of a model that has a closed-form solution. Lastly, based on the findings from this comparison, we suggest modifications to the stochastic extended path approach.

2.1. **Numerical integration.**

2.1.1. *Gaussian quadrature.* Let X be a Gaussian random variable with mean zero and variance $\sigma_x^2 > 0$. We aim to evaluate $\mathbb{E}[\varphi(X)]$, where φ is a continuous function. Calculating the expectation involves evaluating the following integral:

$$\mathbb{E}[\varphi(X)] = \frac{1}{\sigma_x \sqrt{2\pi}} \int_{-\infty}^{\infty} \varphi(x) e^{-\frac{x^2}{2\sigma_x^2}} \mathrm{d}x.$$

which can be approximated using a well-established result (refer to Judd (1998)):

$$\int_{-\infty}^{\infty} \phi(x) e^{-x^2} \mathrm{d}x = \sum_{i=1}^{m} \omega_i \phi(x_i) + \frac{m! \sqrt{m}}{2^m} \frac{\phi^{(2m)}(\xi)}{(2m)!}$$

for any $\xi \in \mathbb{R}$. Here, the last term on the right-hand side reflects the approximation error, where x_i (for $i = 1, \ldots, m$) denote the roots of an order m Hermite polynomial, and the weights ω_i are positive. For a specified order of approximation m, the approximation error is proportional to the order $2m$ derivative of the integrand. This result indicates that it is feasible to derive a sequence of weights ω_i such that evaluating the integral using the right-hand side provides exact results for any polynomial of order $2m - 1$. The method described by Golub and Welsch (1969) outlines the process for calculating the quadrature weights and nodes (ω_i, x_i) through the eigenvalues and eigenvectors of a symmetric tridiagonal matrix. A change of variables is required to evaluate $\mathbb{E}[\varphi(X)]$. We set $z = \frac{x}{\sigma_x \sqrt{2}}$ and use the following approximation for the expectation:

$$\mathbb{E}[\varphi(X)] \approx \frac{1}{\sqrt{\pi}} \sum_{i=1}^{m} \omega_i \varphi(z_i).$$

In our models, we often have multiple sources of uncertainty, *i.e.* more than one shock, necessitating consideration of cases where X is a random vector. If X is a multivariate Gaussian random variable, we can employ a tensor product approach. Specifically, if X is defined in $\mathbb{R}^{n_s}$ with $\mathbb{E}[X] = 0$ and $\mathbb{V}[X] = \Sigma$, and $\psi(\mathbf{x})$ is a function mapping $\mathbb{R}^{n_s}$ to $\mathbb{R}^n$, we utilize the following approximation:

$$\mathbb{E}[\psi(X)] = (2\pi)^{-\frac{m}{2}} \Sigma^{-\frac{1}{2}} \int_{\mathbb{R}^m} \psi(\mathbf{x}) e^{-\frac{1}{2}\mathbf{x}'\Sigma^{-1}\mathbf{x}} \mathrm{d}\mathbf{x}$$

$$\approx \pi^{-\frac{m}{2}} \sum_{i_1=1}^{n_s} \sum_{i_2=1}^{n_s} \cdots \sum_{i_m=1}^{n_s} \omega_{i_1} \omega_{i_2} \cdots \omega_{i_m} \psi(z_{i_1}^1, z_{i_2}^2, \ldots, z_{i_m}^m)$$

where we define the change of variables as $\mathbf{z} \equiv (z^1, z^2, \ldots, z^q)' = \Sigma^{-\frac{1}{2}} \mathbf{x}/\sqrt{2}$. A notable limitation of this tensor product rule is that the number of function evaluations for ψ grows exponentially with the dimensionality of X. There is a curse of dimensionality regarding the number of shocks. Computationally more efficient alternatives exist.

2.1.2. *Unscented transforms.* As the number of shocks increases, the Gauss-Hermite formula and tensor products become impractical. An alternative approach is to utilize monomial formulas (refer to Stroud (1971)). Recently, the theory of unscented transforms has revisited this topic, as discussed in Julier, Uhlmann, and Durrant-Whyte (2000) and Julier (2002).

The Unscented Transform is a method used to estimate how a probability distribution evolves under a nonlinear mapping. Essentially, it provides a means to approximate an integral involving a nonlinear function of a random variable without depending on quadrature methods or Monte Carlo simulations. This technique has been developed within the framework of nonlinear filters designed to estimate nonlinear state space models. Julier, Uhlmann, and Durrant-Whyte (2000) present an appealing and cost-effective method for integration in $\mathbb{R}^{n_s}$, utilizing a formula that involves $2n_s + 1$ nodes, referred to as sigma points in the literature. Defining the matrix P such that $P'P = \Sigma$, the nodes are given by:

$$\begin{cases} x_1 = 0 \\ x_i = \sqrt{n_s + \kappa P_i} & \text{for } i = 1, \ldots, n_s \\ x_i = -\sqrt{n_s + \kappa P_i} & \text{for } i = n_s + 1, \ldots, 2n_s + 1 \end{cases}$$

where κ is a positive real scaling parameter. The corresponding weights are defined as:

$$\begin{cases} \omega_1 = \frac{\kappa}{m+\kappa} \\ \omega_i = \frac{1}{2(m+\kappa)} & \text{for all } i > 1 \end{cases}$$

The unscented transformation allows us to accurately recover the mean and covariance matrix for any third-order polynomial function of X. The adjustable parameter κ can be utilized to align with other moments or characteristics of the distribution of $\varphi(X)$.

2.2. **Trees of possible futures.** Given a set of weights and nodes $(\omega_i, \epsilon_i)_{i=1}^m$ where m is odd, ensuring that $\epsilon_1 = 0$ serves as the central node, we construct a stochastic extended path simulation of order 1 by substituting the auxiliary perfect foresight model, as detailed in equation (2), with:

$$
\sum_{i=1}^{m} \omega_i f\left(y_{t-1}, y_t, y_{t+1}^i, \varepsilon_t\right) = 0
$$

(3)

$$
\Big|_{i=1,\dots,m} \begin{bmatrix} f\left(y_t, y_{t+1}^i, y_{t+2}^i, \epsilon_i\right) = 0 \\ f\left(y_{t+1}^i, y_{t+2}^i, y_{t+3}^i, 0\right) = 0 \\ \vdots \\ f\left(y_{t+H-2}^i, y_{t+H-1}^i, y^\star, 0\right) = 0 \end{bmatrix}
$$

in the main loop of the extended path algorithm 1. The initial block of n rows serves to approximate the conditional expectation for period t. Following this block, there are m deterministic trajectories leading to the steady state. For each shock state ϵ in period $t+1$, we must solve a perfect foresight problem over $H-2$ periods, akin to the formulation presented in equation (2). It is important to recognize that these problems cannot be treated in isolation due to their shared initial condition, y_t, which remains to be determined. Given that all possible futures share a common history (y_{t-1}, which is predetermined, and y_t, which will be determined as part of the solution to the system of equations (3)), we cannot simply derive y_t by averaging m perfect foresight simulations in parallel[5].

This system of equations is larger than the one addressed in section 1.1, comprising $n + nm(H-1)$ equations compared to the nH equations of the perfect foresight model. Nevertheless, we can still apply a similar Newton-based approach to tackle the auxiliary model. It is important to note, however, that the Jacobian matrix of the stacked equations is no longer block tridiagonal.

Obviously, we would like to go further by approximating the conditional expectations over the first p periods.

---

[5]It is indeed feasible to explicitly parallelize the solution algorithm by utilizing nested Newton solvers. For a specified value of y_t, we can concurrently solve the m perfect foresight models, employing the strategy outlined in section 1.1. Subsequently, we only need to determine y_t using another Newton-type algorithm that integrates the parallelized solvers for the periods spanning from $t+1$ to $t+H-1$. We did not explore this possibility as we found the direct approach to be simpler; however, this strategy may prove beneficial as the model scales, either due to the complexity of the model itself or an increased number of integration nodes.

2.2.1. *Future as a perfect m-ary tree.* The most obvious way to account for future uncertainty between t and $t+p$ is to consider all the possible sequences of discretized shocks on p periods. This correspond to a perfect m-ary tree. Figure 1 represent such a tree for the second order stochastic extended path. The m-ary tree's leaves are zero shock trajectories between periods $t+p+1$ and $t+H-1$ of the auxiliary model. Integral approximations for conditional expectations are calculated at each node of the tree, except for the terminal nodes where we revert to a standard perfect foresight model.

At the base of the tree, corresponding to period t of the auxiliary model, we must have:

$$(4.a) \qquad \sum_{i_1=1}^{m} \omega_{i_1} f\left(y_{t-1}, y_t, y_{t+1}^{i_1}, \varepsilon_t\right) = 0$$

Moving to the first level of the tree, representing period $t+1$ of the auxiliary model, we must satisfy the following m equations, one for each node:

$$(4.b) \qquad \sum_{i_2=1}^{m} \omega_{i_2} f\left(y_t, y_{t+1}^{i_1}, y_{t+1}^{i_2,i_1}, \epsilon_{i_1}\right) = 0 \ \forall i_1 \in \{1,\dots,m\}$$

In the second level of the tree, we encounter m^2 equations that must be fulfilled:

$$(4.c) \qquad \sum_{i_3=1}^{m} \omega_{i_3} f\left(y_{t+1}^{i_1}, y_{t+2}^{i_2,i_1}, y_{t+3}^{i_3,i_2,i_1}, \epsilon_{i_2}\right) = 0 \ \forall (i_1,i_2) \in \{1,\dots,m\}^2$$

This process continues up to level $p-1$ of the tree, where m^{p-1} equations must similarly be satisfied:

$$(4.d) \qquad \sum_{i_p=1}^{m} \omega_{i_p} f\left(y_{t+p-2}^{i_{p-2},\dots,i_1}, y_{t+p-1}^{i_{p-1},\dots,i_1}, y_{t+p}^{i_p,\dots,i_1}, \epsilon_{i_{p-1}}\right) = 0 \ \forall (i_1,\dots,i_{p-1}) \in \{1,\dots,m\}^{p-1}$$

Subsequently, starting from the terminal nodes of the m-ary tree of height p, we must resolve m^p perfect foresight problems over $H-p-1$ periods:

$$(4.e) \qquad \begin{aligned} &f\left(y_{t+p-1}^{i_{p-1},\dots,i_1}, y_{t+p}^{i_p,\dots,i_1}, y_{t+p+1}^{i_p,\dots,i_1}, \epsilon_{i_p}\right) = 0 \ \forall (i_1,\dots,i_p) \in \{1,\dots,m\}^p \\ &f\left(y_{t+p}^{i_p,\dots,i_1}, y_{t+p+1}^{i_p,\dots,i_1}, y_{t+p+2}^{i_p,\dots,i_1}, 0\right) = 0 \ \forall (i_1,\dots,i_p) \in \{1,\dots,m\}^p \\ &\quad\vdots \\ &f\left(y_{t+H-2}^{i_p,\dots,i_1}, y_{t+H-1}^{i_p,\dots,i_1}, y^\star, 0\right) = 0 \ \forall (i_1,\dots,i_p) \in \{1,\dots,m\}^p \end{aligned}$$

The system of equations (4.a)–(4.e), similar to the first-order stochastic extended path auxiliary model (3), is inherently non-separable. However, it can still be solved, in principle, through the application of a Newton-based algorithm. However, the number

of unknown vectors y grows exponentially with p and polynomially with m. The total number of unknown vectors of size $n \times 1$ can be expressed as follows:

$$
\begin{aligned}
\mathcal{C}^\star(m, p, H) &= 1 + m + m^2 + \cdots + m^{p-1} + m^p(H - p) \\
&= \frac{m^p - 1}{m - 1} + m^p(H - p)
\end{aligned}
$$

This indicates that the size of the linear system to be solved in each iteration of the Newton algorithm is given by $n\mathcal{C}^\star(m, p, H)$. Moreover, the Jacobian matrix is sparse, and the total number of non-zero $n \times n$ blocks[6] can be computed as:

$$
\text{nnz}^\star(m, p, H) = 1 + m + (2 + m)\frac{m^p - m}{m - 1} + 3m^p(H - p) - m^p
$$

As a result, the ratio of non-zero blocks to the overall number of blocks, indicated by $\mathcal{C}^{\star 2}$, tends to diminish towards zero as either m or p increases. Figure 3 illustrates the distribution of the non-zero $n \times n$ blocks within the stacked Jacobian matrix for the scenario where $p = 2$ and $m = 3$. In practical applications involving this tree structure, we can only consider moderate orders of the stochastic extended path algorithm.

2.2.2. *Sparse tree of future innovations.* Employing the perfect m-ary tree presented above is infeasible for large values of p or m. Trimming the tree by eliminating branches with low probabilities (as determined by the products of quadrature weights) offers limited benefits, as the pruned tree would still expand exponentially with respect to p.

The trunk of the m-ary tree is defined by traversing the central nodes from one period to the next, which happen to be the nodes evaluating to zero[7]. We develop a sparse tree structure by eliminating branches that do not directly emerge from the trunk. This fishbone-shaped sparse tree features a linear growth in the number of nodes with respect to p or m. This framework is analogous to a monomial rule, where innovations occurring in various periods are regarded as separate shocks. Figure 2 illustrates this sparse tree in the context of the second-order stochastic extended path.

Let Let $y_{t,s}^i$ represent the vector of endogenous variables at time $s > t$ along a branch that diverges from the trunk at time t due to the anticipated shock (integration node) ϵ_i. The sequence y_t (at the base of the tree), $y_{t,t+1}^1$, $y_{t+1,t+2}^1$, ..., $y_{t+p-1,t+p}^1$ represents the path of the endogenous variables along the trunk. All the approximate integrals are located along the trunk.

At the base of the tree, corresponding to period t of the auxiliary model, we have the following condition:

---

[6]Typically, these blocks are sparse matrices themselves, as not all variables appear in every equation within a standard model.

[7]In the case of Gaussian quadrature we consider an odd number of nodes.

(5.a)
$$\sum_{i=1}^{m} \omega_i f\left(y_{t-1}, y_t, y_{t,t+1}^i, \varepsilon_t\right) = 0$$

This equation mirrors the one found at the base of a perfect m-ary tree. Advancing to the first level of the tree, which represents period $t+1$ of the auxiliary model, we encounter the following system of m equations that must be satisfied:

(5.b)
$$\begin{cases} \sum_{i=1}^{m} \omega_i f\left(y_t, y_{t,t+1}^1, y_{t+1,t+2}^i, \epsilon_1\right) = 0 \\ f\left(y_t, y_{t,t+1}^i, y_{t,t+2}^i, \epsilon_i\right) = 0 \quad \forall i \in \{2, \ldots, m\} \end{cases}$$

Here, ϵ_1, the central integration node, is equal to zero. Moving to the second level of the tree, we now have $2(m-1)+1$ equations to solve:

(5.c)
$$\begin{cases} \sum_{i=1}^{m} \omega_i f\left(y_{t,t+1}^1, y_{t+1,t+1}^1, y_{t+2,t+3}^i, \epsilon_1\right) = 0 \\ f\left(y_{t,t+1}^i, y_{t,t+2}^i, y_{t,t+3}^i, 0\right) = 0 \quad \forall i \in \{2, \ldots, m\} \\ f\left(y_{t,t+1}^1, y_{t+1,t+2}^i, y_{t+1,t+3}^i, \epsilon_i\right) = 0 \quad \forall i \in \{2, \ldots, m\} \end{cases}$$

At level $h < p$, corresponding to period $t+h$ of the auxiliary model, we have system of $h(m-1)+1$ equations:

(5.d)
$$\begin{cases} \sum_{i=1}^{m} \omega_i f\left(y_{t+h-2,t+h-1}^1, y_{t+h-1,t+h}^1, y_{t+h,t+h+1}^i, \epsilon_1\right) = 0 \\ f\left(y_{t,t+h-1}^i, y_{t,t+h}^i, y_{t,t+h+1}^i, 0\right) = 0 \quad \forall i \in \{2, \ldots, m\} \\ f\left(y_{t+1,t+h-1}^i, y_{t+1,t+h}^i, y_{t+1,t+h+1}^i, 0\right) = 0 \quad \forall i \in \{2, \ldots, m\} \\ \vdots \\ f\left(y_{t+h-2,t+h-1}^1, y_{t+h-1,t+h}^i, y_{t+h-1,t+h+1}^i, \epsilon_i\right) = 0 \quad \forall i \in \{2, \ldots, m\} \end{cases}$$

In level p, we do not compute approximate integrals and are only addressing deterministic problems, which results in a system comprising $p(m-1)+m$ equations:

(5.e)
$$\begin{cases} f\left(y_{t+p-2,t+p-1}^1, y_{t+p-1,t+p}^i, y_{t+p-1,t+p+1}^i, \epsilon_i\right) = 0 \quad \forall i \in \{1, \ldots, m\} \\ f\left(y_{t,t+p-1}^i, y_{t,t+p}^i, y_{t,t+p+1}^i, 0\right) = 0 \quad \forall i \in \{2, \ldots, m\} \\ f\left(y_{t+1,t+p-1}^i, y_{t+1,t+p}^i, y_{t+1,t+p+1}^i, 0\right) = 0 \quad \forall i \in \{2, \ldots, m\} \\ \vdots \\ f\left(y_{t+p-2,t+p-1}^i, y_{t+p-1,t+p}^i, y_{t+p-1,t+p+1}^i, 0\right) = 0 \quad \forall i \in \{2, \ldots, m\} \end{cases}$$

Finally, for all subsequent periods of the auxiliary model up to period $t+H-1$, we establish the following conditions for $h = p+1, \ldots, H$:

(5.f)
$$\begin{cases} f\left(y^i_{t,t+h-1}, y^i_{t,t+h}, y^i_{t,t+h+1}, 0\right) = 0 & \forall i \in \{2, \dots, m\} \\ f\left(y^i_{t+1,t+h-1}, y^i_{t+1,t+h}, y^i_{t+1,t+h+1}, 0\right) = 0 & \forall i \in \{2, \dots, m\} \\ \vdots \\ f\left(y^i_{t+h-2,t+h-1}, y^i_{t+h-1,t+h}, y^i_{t+h-1,t+h+1}, 0\right) = 0 & \forall i \in \{1, \dots, m\} \end{cases}$$

In the last block of equations, $y_{t+H} = y^\star$ in the period $t + H - 1$ of the auxiliary model. As in section 2.2.1 this system of nonlinear equations can be solved with a Newton-based algorithm. The number of unknown $n \times 1$ vectors to be solved for is:

$$\mathcal{C}(m, p, H) = H + \sum_{i=1}^{p} (m-1)(H-i)$$
$$= (1 + (m-1)p) H - \frac{p(p+1)}{2}$$

The number of non zero $n \times n$ blocks in the stacked Jacobian is:

$$\text{nnz}(m, p, H) = \underbrace{\overbrace{3H - 2}^{\text{EP}} + \overbrace{(m-1)p}^{\substack{\text{Approximate} \\ \text{integrals}}}}_{\text{Along the trunk}} + (m-1) \sum_{i=1}^{p-1} (3(H-1-i) + 2)$$

Compared to section 2.2.1 with a perfect m-ary tree, the Jacobian matrix is smaller in size, with its growth occurring linearly with respect to p or m; however, it also is denser. As in section 2.2.1, the proportion of non zero blocks in the Jacobian matrix converges to zero as p tends to infinity. Figure 4 illustrates the distribution of the non-zero $n \times n$ blocks within the stacked Jacobian matrix for the scenario where $p = 2$ and $m = 3$.

2.3. **Accuracy of the Stochastic extended path approach.** To assess the accuracy of the stochastic extended path approach, we follow Collard and Juillard (2001) and examine the asset pricing model introduced by Burnside (1998). This model is particularly relevant here as it generates a significant difference between the deterministic steady state and the unconditional expectation, in this sense future uncertainty matters. It also has the advantage, as shown by Burnside (1998), of having a closed-form solution. We can therefore assess approximation errors by comparing simulations with the stochastic extended path approach and simulations based on the exact solution. We do not claim that this model should be simulated using our approach, as perturbation is significantly more efficient. We consider this model solely to assess our approach's capability to address future uncertainty[8].

Burnside (1998) shows, considering an endowment economy with a growth rate of dividends modelled as a gaussian AR(1), that the price-dividend ratio, v_t, obeys the

---

[8]Utilizing the stochastic extended path approach is reasonable only when the model exhibits significant nonlinearities, features occasionally binding constraints, or deviates substantially from its steady state.

following equations:

$$\begin{cases} v_t = \beta\mathbb{E}_t \left[e^{(1-\gamma)x_{t+1}} (1 + v_{t+1}) \right] \\ x_t = (1-\rho)\mu + \rho x_{t-1} + \varepsilon_t \end{cases}$$

where x_t is the growth rate of dividends, ε_t is a gaussian white noise, β a discount factor and $1/\gamma$ the elasticity of intertemporal substitution. Iterating forward on v_t we find that v_t is a discounted sum of conditional expectations of log-normal random variables. Burnside (1998) shows that the exact solution for v_t is:

$$v_t = \sum_{i=1}^{\infty} \beta^i e^{a_i + b_i(x_t - \mu)}$$

where:

$$a_i = (1-\gamma)\mu i + \frac{(1-\gamma)^2\sigma^2}{2(1-\rho)^2} \left(i - 2\rho\frac{1-\rho^i}{1-\rho} + \rho^2\frac{1-\rho^{2i}}{1-\rho^2} \right)$$

and

$$b_i = \frac{(1-\gamma)\rho \left(1-\rho\right)^i}{1-\rho}$$

The deterministic steady state is obtained by setting $x_t = \mu$ and $\sigma^2 = 0$:

$$v^\star = \sum_{i=1}^{\infty} e^{(1-\gamma)\mu i}$$

and one can easily show that the unconditional expectation of the price-dividend ratio is:

$$\mathbb{E}\left[v_t\right] = \sum_{i=1}^{\infty} \beta^i e^{a_i + \frac{1}{2}\frac{b_i^2\sigma^2}{1-\rho^2}} > v^\star$$

Considering the benchmark calibration utilized in Collard and Juillard (2001) and Burnside (1998), we obtain $y^\star \approx 12.3035$ and $\mathbb{E}\left[v_t\right] \approx 12.4815$. By incorporating future uncertainty, we determine that the unconditional expectation exceeds the deterministic steady state by 1.4466%[9]. Is it possible to account for this gap using the stochastic extended path approach?

---

[9]Alternatively, we can compare the deterministic steady state with the risky steady state, which assumes the absence of current shocks while acknowledging the possibility of future shocks:

$$\tilde{v} = \sum_{i=1}^{\infty} \beta^i e^{a_i}$$

This value would be approximately equal to 12.4812 based on our calibration.

	P1	P2	EP	SEP*(2)	SEP(2)
$100 \times \mathrm{mean}(|\hat{v}_t - v_t|/v_t)$	1.4261	0.0193	1.4241	1.2206	1.2532
$100 \times \min(|\hat{v}_t - v_t|/v_t)$	1.4239	0.0000	1.4236	1.2202	1.2509
$100 \times \max(|\hat{v}_t - v_t|/v_t)$	1.4707	0.0527	1.4250	1.2215	1.2542

TABLE 1. **Comparison with the true solution.** Columns P1 and P2 present the deviations from the true solution for first and second order perturbations. EP denotes the extended path (which assumes no future uncertainty), while the SEP* and SEP columns correspond to the second order stochastic extended path, using a perfect tree and a sparse tree, respectively.

We constructed Table 1 by simulating the model using the true solution, terminating the infinite sum after 800 periods, and comparing these "true data" with simulations generated via perturbation and stochastic extended path methods. As anticipated, the extended path simulations closely resemble those produced by a first-order approximation around the steady state. While the accuracy errors are marginally lower with the extended path approach, both methodologies operate under certainty equivalence. The second-order stochastic extended path, whether implemented through a perfect tree or a sparse tree, demonstrates notable improvements compared to the extended path method. However, we still observe a significant gap in accuracy compared to the local second-order approximation around the deterministic steady state. Our analysis indicates that accuracy errors diminish as the order of approximation in the stochastic extended path increases; however, the improvement tends to be rather slow as the approximation order increases. In conclusion, a notable characteristic of the accuracy errors associated with (S)EP is their significantly lower volatility compared to those derived from perturbation methods, as evidenced by the difference between the minimum and maximum errors. This observation suggests that the erros do not depend much on the state of the economy and that the component we are overlooking remains relatively constant.

What order of approximation is necessary to beat the second-order perturbation or to obtain an unconditional expectation for v that is closer to its true value? To establish a lower bound, we can analytically compute the unconditional expectation of v when utilizing the stochastic extended path approach, assuming that there are no accuracy errors in the quadratures employed at each node of the tree representing future histories.[10] For the extended path we have:

$$v_t^{(0)} = \sum_{i=1}^{\infty} \beta^i e^{a_i^{(0)} + b_i(x_t - \mu)}$$

with

$$a_i^{(0)} = (1 - \gamma)\mu i$$

---

[10] We calculate the exact solution of the asset pricing model under the assumption that non-zero future shocks will occur solely within the next p periods.

so that the unconditional expectation is:

$$\mathbb{E}\left[v_t^{(0)}\right] = \sum_{i=1}^{\infty} \beta^i e^{a_i^{(0)} + \frac{1}{2} \frac{b_i^2 \sigma^2}{1-\rho^2}} < \mathbb{E}\left[v_t\right]$$

With our calibration, we calculate that $\mathbb{E}\left[v_t^{(0)}\right] \approx 12.3038$, which represents a reduction of approximately 1.4239% compared to the true unconditional expectation. More generally, for an approximation of order p, we have:

$$v_t^{(p)} = \sum_{i=1}^{\infty} \beta^i e^{a_i^{(p)} + b_i(x_t - \mu)}$$

with

$$a_i^{(p)} = (1-\gamma)\mu i + \begin{cases} \frac{(1-\gamma)^2 \sigma^2}{2(1-\rho)^2} \left(i - 2\rho \frac{1-\rho^i}{1-\rho} + \rho^2 \frac{1-\rho^{2i}}{1-\rho^2}\right) & \text{if } i \leq p \\ \frac{(1-\gamma)^2 \sigma^2}{2(1-\rho)^2} \left(p - 2\rho \frac{\rho^{i-p} - \rho^i}{1-\rho} + \rho^2 \frac{\rho^{2(i-p)} - \rho^{2i}}{1-\rho^2}\right) & \text{otherwise.} \end{cases}$$

so that the unconditional expectation is:

$$\mathbb{E}\left[v_t^{(p)}\right] = \sum_{i=1}^{\infty} \beta^i e^{a_i^{(p)} + \frac{1}{2} \frac{b_i^2 \sigma^2}{1-\rho^2}} < \mathbb{E}\left[v_t\right]$$

Table 2 illustrates the extent to which the gap between the exact unconditional expectation, $\mathbb{E}\left[v_t\right]$, and the unconditional expectation derived from extended path simulation, $\mathbb{E}\left[v_t^{(0)}\right]$, is narrowed as we incorporate various orders of the stochastic extended path. To effectively capture the impacts of future uncertainty in our calibration, a large value of p is essential. In this regard, the perturbation approach proves to be considerably more efficient.

p	Contribution in %
1	7.55
10	53.81
20	78.63
40	95.43
60	99.02
80	99.79
100	99.95
120	99.99
140	100.00

TABLE 2. **Future uncertainty accounting.** The second column presents the proportion of the gap between $\mathbb{E}\left[v_t\right]$ and $\mathbb{E}\left[v_t^{(0)}\right]$, as attributable to different orders of the stochastic path.

2.4. **An hybrid approach.** Capturing the full effect of future volatility would, in principle, require a high-order stochastic extended path. On the other hand, the perturbation approach provides an alternative and more accurate approximation of the effects of future volatility. The idea behind the hybrid stochastic extended path is to combine the treatment of important nonlinearities in the model (via the stochastic extended path method) with a broader treatment of future volatility effects (via a perturbation approach).

Let us introduce σ, called the *stochastic scale* of the model, such that

$$\varepsilon_{t+1} = \sigma \eta_{t+1}$$

where η_t is a $n_s \times 1$ gaussian random vector with zero mean and covariance matrix Σ_η. It follows that the covariance of ε_t is then $\Sigma = \sigma^2 \Sigma_\eta$. Consider the (unknown) solution function g:

$$y_t = g\left(y_{t-1}, \varepsilon_t, \sigma\right)$$

so that the original model (1) is satisfied. Plugging g into this model, we obtain:

$$\mathbb{E}_t \mathcal{F}\left(y_{t-1}, \varepsilon_t, \eta_{t+1}, \sigma\right) = \mathbb{E}_t f\left(y_{t-1}, g\left(y_{t-1}, \varepsilon_t, \sigma\right), g\left(g\left(y_{t-1}, \varepsilon_t, \sigma\right), \sigma, \eta_{t+1}, \sigma\right), \varepsilon_t\right) = 0$$

From the perspective of the expectation operator $\mathbb{E}_t$, η_{t+1} is the relevant source of uncertainty.

The *hybrid stochastic extended path* approach considers a Taylor expansion of $\mathcal{F}$ in the sole direction of σ. That is, we expand $\mathbb{E}_t f(\cdot)$ in powers of σ:

$$\mathbb{E}_t \mathcal{F}\left(y_{t-1}, \varepsilon_t, \eta_{t+1}, \sigma\right) = f\left(y_{t-1}, g\left(y_{t-1}, \varepsilon_t, 0\right), g\left(g\left(y_{t-1}, \varepsilon_t, 0\right), 0, 0, 0\right), \varepsilon_t\right)$$
$$+ \mathbb{E}_t\left[\sum_{i=1}^{\infty} \frac{1}{i!} \frac{\partial^i \mathcal{F}}{\partial \sigma^i} \sigma^i\right]$$

If we consider a full tree of future histories, in the first p periods of the stochastic extended path, the quadrature method includes both deterministic effects and future volatility. After these first p periods, starting in period $t + p - 1$, the deterministic solution (with zero shocks) corresponds to the leading term of the above expansion. A perturbation expansion in the direction of σ can correct for longer-run volatility effects after period $t + p - 1$. We maintain the terminal condition of the auxiliary model, ensuring that each leaf converges to the deterministic steady state at the end..

Specifically, in the deterministic problems at the terminal nodes[11], we adjust the expected values for period $t + h + 1$, which are incorporated into the problem for period $t + h$, as follows:

$$\widetilde{y}_{t+h+1} = y_{t+h+1} + \frac{1}{2} g_{\sigma^2}$$

---

[11]In the case of a perfect m-ary tree, there are m^p such problems at period $t + p$ of the auxiliary model. In a sparse tree, there are $(m - 1)$ problems in each of the periods $t + 1, \ldots, p - 1$ and m problems in period $t + p$ of the auxiliary model.

where g_{σ^2} is the second derivative of the solution function with respect to σ evaluated at $\sigma = 0$.

	SEP*(2)	SEP(2)	SEP*(2+)	SEP(2+)	SEP(2++)
$100 \times \text{mean}(|\hat{v}_t - v_t|/v_t)$	1.2206	1.2532	0.0162	0.0163	0.0004
$100 \times \text{min}(|\hat{v}_t - v_t|/v_t)$	1.2202	1.2529	0.0155	0.0153	0.0000
$100 \times \text{max}(|\hat{v}_t - v_t|/v_t)$	1.2215	1.2542	0.0173	0.0177	0.0014

TABLE 3. **Comparison with the true solution.** The columns SEP*(2) and SEP(2) represent the second order stochastic extended paths, utilizing both a perfect tree and a sparse tree. In contrast, the columns SEP*(2+) and SEP(2+) correspond to their hybrid versions (based on a second order approximation of the model). The final column, SEP(2 + +), represents the second-order stochastic extended path with a sparse tree; however, the hybrid correction relies on a fourth-order approximation of the model.

Table 3 illustrates that the hybrid version markedly diminishes accuracy errors. In fact, the accuracy errors are even lower than those found in the second-order perturbation case. The maximum error with a hybrid second-order stochastic extended path is less than half the maximum error obtained with second-order perturbation. Furthermore, additional unreported figures show a gradual decrease in accuracy errors as the order of the stochastic extended path increases.

We can improve the accuracy of the hybrid stochastic extended path by incorporating higher-order perturbation corrections. The final column of Table 3 illustrates that substituting $\frac{1}{2}g_{\sigma^2}$ with the correction to the constant derived from fourth-order perturbation significantly improves precision.. In this context, pursuing a sixth-order (or higher) local approximation would not yield significant benefits. The main reason for this is that the default tolerance parameter of 1×10^{-5}, used by the nonlinear solvers in Dynare, should be reduced to observe notable differences in the simulated data, albeit at the expense of additional iterations in the Newton solver.

Thus, the *hybrid stochastic extended path* approach merges two strategies:

(1) A stochastic extended path method of order p to handle large short-run non-linearities and occasionally binding constraints (such as a zero lower bound).

(2) A perturbation-based correction, capturing how uncertainty well beyond p periods contributes to the current state via higher-moment.

By adopting this approach, we maintain the essential benefits of the extended path method for managing significant nonlinearities in the short term, while employing perturbation techniques to account for the average effects of random fluctuations over

the longer term, all without excessively increasing the complexity of the underlying system of equations.

3. Numerical illustration

Employing the stochastic extended path approach is justifiable primarily when the model exhibits significant deterministic nonlinearities, as seen in scenarios involving Occasionally Binding Constraints, or when the model is permitted to deviate substantially from its deterministic steady state. As an illustration, we consider a Real Business Cycle model with irreversible investment. The social planner problem is:

$$\max_{\{c_{t+j}, l_{t+j}, k_{t+1+j}\}_{j=0}^{\infty}} \quad \mathcal{W}_t = \sum_{j=0}^{\infty} \beta^j u(c_{t+j}, l_{t+j})$$

$$\underline{s.t.}$$

$$y_t = c_t + i_t$$

$$y_t = A_t f(k_t, l_t)$$

$$k_{t+1} = i_t + (1 - \delta)k_t$$

$$i_t \geq 0$$

$$A_t = A^\star e^{a_t}$$

$$a_t = \rho a_{t-1} + \varepsilon_t$$

where the technology (f) and the preferences (u) are defined by

$$f(k_t, l_t) = \left(\alpha k_t^{\psi} + (1 - \alpha) l_t^{\psi} \right)^{\frac{1}{\psi}}$$

and

$$u(c_t, l_t) = \frac{\left(c_t^{\theta} (1 - l_t)^{1-\theta} \right)^{1-\tau}}{1 - \tau}$$

The innovation term ε_t is modeled as Gaussian white noise with a mean of zero and a variance of σ_{ε}^2. This framework presents a compelling scenario due to the presence of two key sources of non-linearity: (*i*) The functional forms related to technology and preferences can be rendered arbitrarily non-linear, for instance, by reducing the elasticity of output in relation to capital, represented as $\frac{1}{1-\psi}$; and (*ii*) An occasionally binding constraint on investment is incorporated into the model. The first order conditions are given by[12]:

$$u_c(c_t, l_t) - \mu_t = \beta \mathbb{E}_t \left[u_c(c_{t+1}, l_{t+1}) \left(A_{t+1} f_k(k_{t+1}, l_{t+1}) + 1 - \delta \right) - \mu_{t+1}(1 - \delta) \right]$$

$$-\frac{u_l(c_t, l_t)}{u_c(c_t, l_t)} - A_t f_l(k_t, l_t) = 0$$

$$c_t + k_{t+1} - A_t f(k_t, l_t) - (1 - \delta)k_t = 0$$

$$\mu_t \left(k_{t+1} - (1 - \delta)k_t \right) = 0$$

---

[12]See annex A.

where μ_t is the Lagrange multiplier associated to the positiveness constraint on investment. This model is exclusively considered for evaluating our simulation approach. Our calibration does not have quantitative objectives; rather, it has been designed to ensure that the economy reaches the minimum investment threshold while undergoing significant deviations from the deterministic steady state. The discount factor is $\beta = 0.990$, the preference parameters θ and τ are respectively equal to 0.357 and 2.000. The technology parameters α and ψ are respectively equal to 0.450 and -0.200. The depreciation rate is $\delta = 0.010$. Finally, the parameters governing TFP are $\rho = 0.800$, $A^\star = 1$ and $\sigma = 0.100$.

Figure 5 presents the results of stochastic extended path simulations for investment across various approximation orders ($p = 0, 1, \ldots, 10$), specifically focusing on the model without a positivity constraint on investment. Notably, we observe substantial fluctuations around the deterministic steady state, with investment values occasionally dropping into negative territory during certain intervals. Incorporating future uncertainty does not alter the outcomes in this particular model. The stochastic nonlinearity is entirely masked by the deterministic nonlinearity resulting from the very large fluctuations. In contrast, Figure 6 illustrates the results obtained from applying the same set of innovations to a model characterized by irreversible investment. We can now discern variations in the outcomes produced by the stochastic extended path algorithm as the approximation order changes. These differences remain minimal when the economy is significantly above the steady state, but they tend to increase as we approach or fall below that steady state. A noteworthy observation is that all the paths maintain a consistent order based on the approximation order p. As we incorporate greater consideration for future uncertainty, the level of investment correspondingly rises. As the order of approximation increases, the likelihood of reaching the lower bound on investment diminishes. Figure 7 illustrates the results of our simulations conducted on a subsample where the constraint on investment is actively binding. The employs figure a gradient color scheme ranging from black to red to denote the progression of the approximation order from 0 to 10. Notably, we observe that the discrepancies arising from increasing the approximation order p diminish as p increases. In fact, the differences between investments simulated at orders 8 and 9, as well as those at orders 9 and 10, are barely discernible.This suggests that a tenth-order approximation using a sparse tree is sufficient to capture the implications of future uncertainty in this model[13].

Conclusion

The stochastic extended path approach offers great versatility and demands little extra effort from a Dynare user, aside from simply writing the model's equations. The tradeoff for this simplicity is that simulating long time series can be quite time-consuming, particularly as we raise the approximation order p.

---

[13]Note also that, for this model, the simulations using the hybrid version of the stochastic extended path would be nearly identical.

A clear application of this approach is that it allows for straightforward verification that the Extended Path method produces accurate simulations for a given model. For example, Section 3 demonstrates that future uncertainty need not be considered in the RBC model when investment is reversible; however, such considerations are essential when investment is irreversible.

One possible extension of this approach lies in its application to estimation. A simple method to consider is the Simulated Method of Moments; however, due to the computational cost of the SEP, which would be further intensified by a simulation-based approach, a conditional likelihood method may prove to be more beneficial. To implement this, we just need to invert the model by identifying the unexpected innovations necessary to align the observed endogenous variables with the data for each period within the sample. If there are k observed variables, this can be achieved by replacing the k observed endogenous variables with k innovations in period t of the auxiliary model.

Université du Mans and Dynare team
Email address: stephane@adjemian.eu

Dynare team
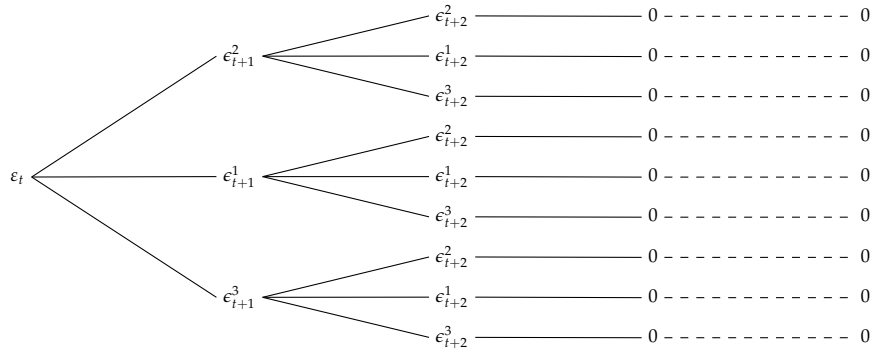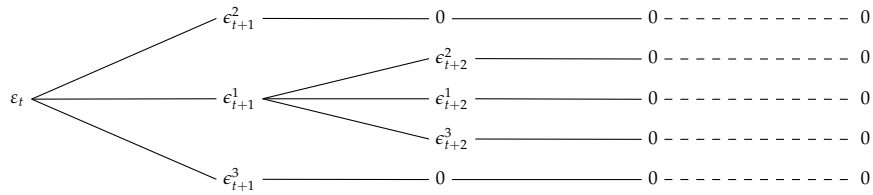*Email address*: michel.juillard@mjui.fr

FIGURE 1. **Paths of future innovations as a perfect tree.** Stochastic extended path of order $p = 2$ with $m = 3$ integration nodes. Perfect ternary tree of length 3, followed by sequences of zeros (the leafs). Conditional expectations are estimated at the root of the tree and at three non-terminal nodes (integration nodes in $t + 1$). The leafs, after the terminal nodes of the perfect tree (integration nodes in $t + 2$), correspond to the deterministic trajectories leading to the steady state for the endogenous variables.

FIGURE 2. **Paths of future innovations as a sparse tree.** Stochastic extended path of order $p = 2$ with $m = 3$ integration nodes. Sparse tree of length 2, followed by sequences of zeros (the leafs). Conditional expectations are estimated along the trunk (here in periods t and $t + 1$). The leafs, after the terminal nodes of the sparse tree (ϵ^2_{t+1}, ϵ^3_{t+1}, ϵ^2_{t+2}, ϵ^1_{t+2} and ϵ^3_{t+2})), correspond to the deterministic trajectories leading to the steady state for the endogenous variables.
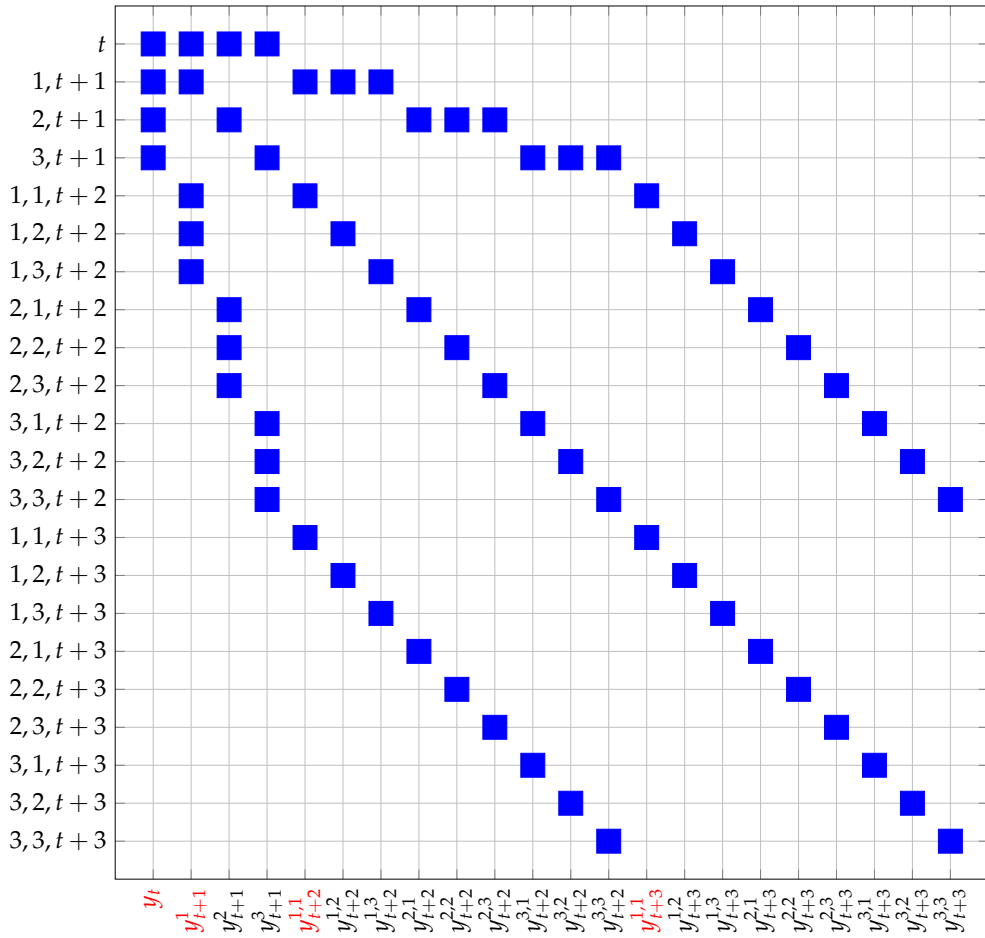
FIGURE 3. **Partial view of the stacked jacobian with a perfect tree.** Stochastic extended path of order $p = 2$ with $m = 3$. We present only the top-left portion of the Jacobian matrix. Each blue square represents a non zero $n \times n$ block of derivatives. The labels on the horizontal axis illustrate the manner in which the unknown vectors are concatenated to construct the stacked system of equations.
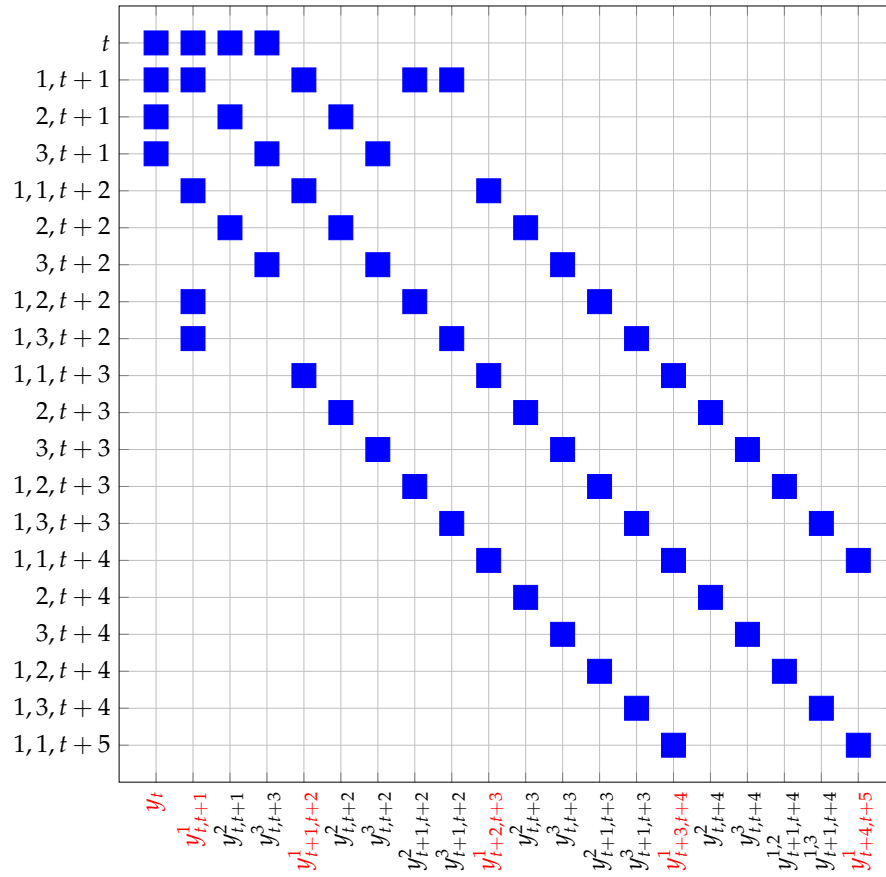
FIGURE 4. **Partial view of the stacked jacobian with a sparse tree.** Stochastic extended path of order $p = 2$ with $m = 3$. We present only the top-left portion of the Jacobian matrix. Each blue square represents a non zero $n \times n$ block of derivatives. The labels on the horizontal axis illustrate the manner in which the unknown vectors are concatenated to construct the stacked system of equations.
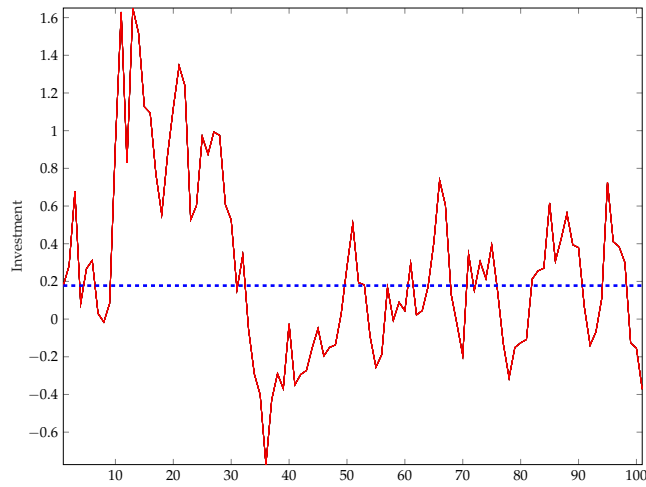
FIGURE 5. **Simulation of the RBC model with reversible investment.**
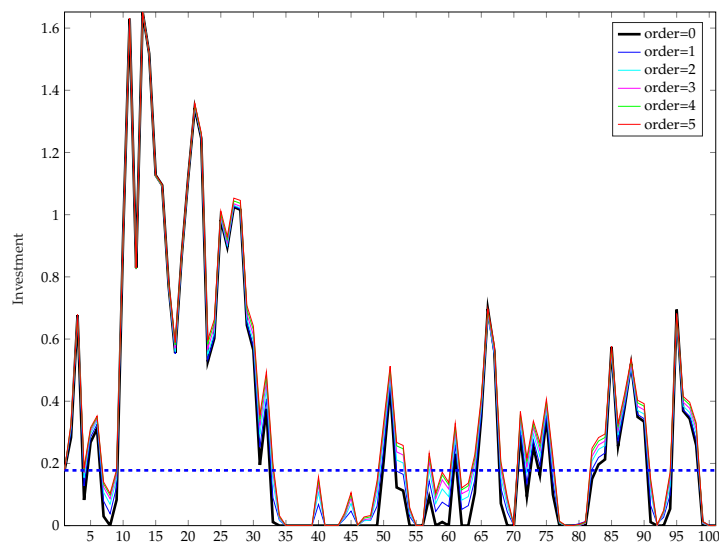Stochastic extended path with orders 0 to 10 (sparse tree).

FIGURE 6. **Simulation of the RBC model with reversible investment.**
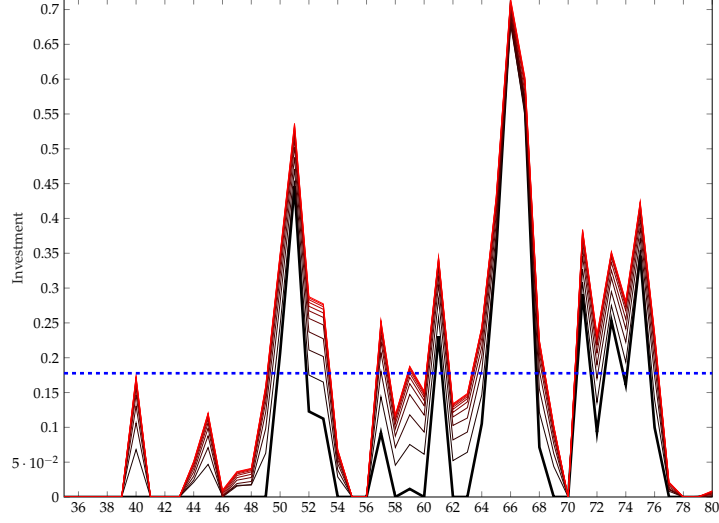Stochastic extended path with orders 0 to 5 (sparse tree).

FIGURE 7. **Simulation of the RBC model with reversible investment.**
Stochastic extended path with orders 0 to 10 (sparse tree).

APPENDIX A. EQUATIONS OF THE RBC MODEL

$$(A.1) \qquad \begin{cases} A_t & = A^\star e^{a_t} \\ a_t & = \rho_a a_{t-1} + u_{a,t} \end{cases}$$

$$
\begin{aligned}
(A.2) \qquad & \left[c_t^\theta (1 - l_t)^{1-\theta} \right]^{-\tau} \theta c_t^{\theta-1} (1 - l_t)^{1-\theta} - \mu_t \\
& - \beta \mathbb{E}_t \Bigg[\left[c_{t+1}^\theta (1 - l_{t+1})^{1-\theta} \right]^{-\tau} \theta c_{t+1}^{\theta-1} (1 - l_{t+1})^{1-\theta} \\
& \times \left\{ \alpha \left[\alpha + (1-\alpha) \left(\frac{k_{t+1}}{l_{t+1}} \right)^{-\psi} \right]^{\frac{1-\psi}{\psi}} A_{t+1} + 1 - \delta \right\} - \mu_{t+1}(1-\delta) \Bigg] = 0
\end{aligned}
$$

$$(A.3) \qquad \frac{1-\theta}{\theta} \frac{c_t}{1 - l_t} - (1-\alpha) A_t \left[\alpha \left(\frac{k_t}{l_t} \right)^\psi + 1 - \alpha \right]^{\frac{1-\psi}{\psi}} = 0$$

$$(A.4) \qquad c_t + k_{t+1} - A_t \left[\alpha k_t^\psi + (1-\alpha) l_t^\psi \right]^{\frac{1}{\psi}} - (1-\delta)k_t = 0$$

$$(A.5) \qquad \mu_t \left(k_{t+1} - (1-\delta)k_t \right) = 0 \text{ with } \mu_t \geq 0 \, \forall t$$

Equations (A.1) define the law of motion for efficiency, where a_t represents the centered logged total factor productivity (TFP). Equation (A.2) presents the Euler equation, while equation (A.3) outlines the first-order condition for labor supply. Equation (A.4) describes the law of motion for the physical capital stock. Finally, equation (A.5) establishes the complementary slackness condition resulting from the investment positivity constraint.

Appendix B. Dynare's equations for the RBC model

Incorporating an occasionally binding constraint into a model with the `extended_path` command is straightforward. This can be achieved by defining a slackness condition within the model block, following the guidelines provided for specifying Mixed Complementarity Problems, as outlined by Adjemian, Juillard, et al. (2024). Below is the `model` block employed to generate figures 5 through 7:

```
1  model(use_dll);
2
3    // Logged TFP
4    efficiency = rho*efficiency(-1) + sigma*epsilon;
5
6    // TFP
7    Efficiency = Effstar*exp(efficiency);
8
9    // Production
10   Output = Efficiency*(alpha*Capital(-1)^psi+(1-alpha)*Labour^psi)^(1/psi);
11
12   // Capital law of motion
13   Capital = Output-Consumption + (1-delta)*Capital(-1);
14
15   // Consumption/Leisure arbitrage
16   (1-theta)/theta*Consumption/(1-Labour) - (1-alpha)*(Output/Labour)^(1-psi);
17
18   // Euler equation
19   (Consumption^theta*(1-Labour)^(1-theta))^(1-tau)/Consumption -
       LagrangeMultiplier =  beta*(Consumption(1)^theta*(1-Labour(1))^(1-theta))
       ^(1-tau)/Consumption(1)*(alpha*(Output(1)/Capital)^(1-psi)+1-delta) +
       LagrangeMultiplier(1)*(1-delta);
20
21   // Investment
22   Investment = Output - Consumption;
23
24   // Lagrange multiplier associated to the positivity constraint on
       investment
25   LagrangeMultiplier = 0 ⊥ Investment > 0;
26
27  end;
```

An arbitrary number of occasionally binding constraints (OBC) can be defined through the same methodology. Employing Dynare's implementation of OccBin, introduced by

Guerrieri and Iacoviello (2015), would prove to be more complex and is restricted to only two constraints. Note that the extended path approach, which does not depend on local approximations unlike OccBin, will yield different simulations unless the model is linear or remains in the vicinity of the deterministic steady state. Full codes are available here:

https://github.com/stepan-a/ep-mj-30-years

References

[1] Stéphane Adjemian and Michel Juillard. *Accuracy of the Extended Path Simulation Method in a New Keynesian Model with Zero Lower Bound on the Nominal Interest Rate*. mimeo. Université du Mans, Feb. 2011.

[2] Stéphane Adjemian, Michel Juillard, et al. *Dynare: Reference Manual, Version 6.* Dynare Working Papers 80. CEPREMAP, Feb. 2024. URL: https://ideas.repec.org/p/cpm/dynare/080.html.

[3] Craig Burnside. "Solving asset pricing models with gaussian shocks". In: *Journal of Economic Dynamics and Control* 22 (1998), pp. 329–340.

[4] Fabrice Collard and Michel Juillard. "Accuracy of stochastic perturbation methods: The case of asset pricing models". In: *Journal of Economic Dynamics and Control* 25.6-7 (2001), pp. 979–999.

[5] Timothy A. Davis. *Direct Methods for Sparse Linear Systems*. Society for Industrial and Applied Mathematics, 2006. ISBN: 0898716136.

[6] Ray C Fair and John B Taylor. "Solution and Maximum Likelihood Estimation of Dynamic Nonlinear Rational Expectations Models". In: *Econometrica* 51.4 (July 1983), pp. 1169–85.

[7] Joseph E. Gagnon. "Solving the Stochastic Growth Model by Deterministic Extended Path". In: *Journal of Business & Economic Statistics* 8.1 (Jan. 1990), pp. 35–36.

[8] H. Golub Gene and H. Welsch John. "Calculation of Gauss Quadrature Rules". In: *Mathematics of Computation* 23 (1969), pp. 221–230.

[9] Luca Guerrieri and Matteo Iacoviello. "OccBin: A toolkit for solving dynamic models with occasionally binding constraints easily". In: *Journal of Monetary Economics* 70.C (2015), pp. 22–38.

[10] Kenneth L. Judd. *Numerical methods in Economics*. MIT press, 1998.

[11] S. Julier. "The scaled unscented transformation". In: *Proceedings of the 2002 American Control Conference (IEEE Cat. No.CH37301)*. Vol. 6. 2002, pp. 4555–4559.

[12] S. Julier, J. Uhlmann, and H.F. Durrant-Whyte. "A new method for the nonlinear transformation of means and covariances in filters and estimators". In: *IEEE Transactions on Automatic Control* 45.3 (2000), pp. 477–482.

[13] Jean-Pierre Laffargue. "Résolution d'un modèle macroéconomique avec anticipations rationnelles". In: *Annales d'Economie et de Statistique* 17 (1990), pp. 97–119.

[14] David R.F. Love. *Accuracy of Deterministic Extended-Path Solution Methods for Dynamic Stochastic Optimization Problems in Macroeconomics*. Working Papers 0907. Brock University, Department of Economics, Nov. 2009.

[15] A. H. Stroud. *Approximate calculation of multiple integrals*. Prentice-Hall, 1971. ISBN: 0130438936.